  Bull. Chem. Soc. Jpn., 53, 2437—2442 (1980)

Studies of the Anodic Oxidation of the Cyanide Ion in the Presence of the Copper Ion. IV. The Kinetics and Mechanism of the Decomposition of the Intermediate Tetracyanocuprate(II) Ion

Seiji Yoshimura, Akira Katagiri,** Yasuo Deguchi,** and Shiro Yoshizawa*

Department of Industrial Chemistry, Faculty of Engineering, Kyoto University, Yoshida, Sakyo-ku, Kyoto 606

***Department of Chemistry, College of Liberal Arts and Sciences, Kyoto University, Yoshida, Sakyo-ku, Kyoto 606*

(Received February 15, 1980)

The kinetics and mechanism of the decomposition of the tetracyanocuprate(II) ion ($Cu^{II}(CN)_4^{2-}$) have been investigated by ESR measurements. Aqueous solutions of potassium cyanide with a small amount of copper(I) cyanide were electrolyzed in a cell the platinum anode of which was set in the resonant cavity of an ESR spectrometer. Since $Cu^{II}(CN)_4^{2-}$, which is formed as an intermediate, gives a definite ESR spectrum, its concentration in the anode compartment is estimated from the intensity of the first-derivative spectrum at a fixed magnetic field. From the decay curves of the ESR intensity after the steady-state electrolysis currents have been switched off, a rate equation for the decomposition of $Cu^{II}(CN)_4^{2-}$ is derived; $v=k_0[Cu^{II}(CN)_4^{2-}]^2/[CN^-]^2$, where k_0 is calculated to be 74 mol·dm^{-3}·s^{-1} at 25 °C. This rate equation is also confirmed by ESR measurements during steady-state electrolysis, where the value of $k_0=60$ mol·dm^{-3}·s^{-1} is obtained. On the basis of the kinetics, two possible mechanisms are proposed: the formation of $Cu^{II}(CN)_3^-$, followed by the rate-determining bimolecular reaction of $Cu^{II}(CN)_3^-$ to give $2Cu^{I}(CN)_2^-+(CN)_2$ (Mechanism A), and the formation of a binuclear complex, $Cu^{II}_2(CN)_6^{2-}$, followed by the rate-determining decomposition of $Cu^{II}_2(CN)_6^{2-}$ to give $2Cu^{I}(CN)_2^-+(CN)_2$ (Mechanism B). The kinetics and the mechanism are compared with those of the chemical reaction between the copper(II) ion and the cyanide ion.

In our previous investigations of the anodic oxidation of the cyanide ion in the presence of the copper ion, we have proposed the following catalytic mechanism:[2,3]

$$Cu^{I}(CN)_4^{3-} \longrightarrow Cu^{II}(CN)_4^{2-} + e^- \quad (1)$$

$$Cu^{II}(CN)_4^{2-} + CN^- \longrightarrow Cu^{I}(CN)_4^{3-} + \frac{1}{2}(CN)_2 \quad (2)$$

We have detected the intermediate tetracyanocuprate (II) ion ($Cu^{II}(CN)_4^{2-}$) by ESR measurement.[1] However, the rate of the chemical reaction, Eq. 2, was too high to be measured by chronopotentiometry or by the rotating-electrode technique under the conditions adopted.[2] In the present work, the kinetic behavior of the intermediate $Cu^{II}(CN)_4^{2-}$ have been investigated by ESR measurement, and the mechanism of the reaction, Eq. 2, discussed.

Experimental

ESR measurement was made by use of a JEOL JES-ME-3X spectrometer with X-band microwave and with a field-modulation frequency of 100 kHz. A cylindrical resonant cavity of the TE_{011} mode was used.

Figure 1 shows the electrolysis cell used. The cell was made from a quartz-glass tube (0.72 mmϕ in inner diameter) and was equipped coaxially with the platinum-wire anode (0.4 mmϕ). A platinum plate was used as the cathode. The effective surface area of the anode was controlled by means of a polyethylene sheath, as is shown in the right-hand part of Fig. 1. The cell was fixed in the spectrometer so that the working anode was positioned at the center of the resonant cavity. All experiments were made at a constant temperature of 25 °C.

The electrolytic solutions were prepared from reagent-grade potassium cyanide and copper(I) cyanide. No supporting electrolyte was used, because the concentration of cyanide was sufficiently high. The concentrations are expressed in the unit of 1 M=1 mol·dm^{-3} throughout this paper. Copper(I) must have been present almost entirely as $Cu^{I}(CN)_4^{3-}$ under the experimental conditions in this work, as can be calculated from the formation constants of the cyano copper(I) complexes.[4] Therefore, the concentration of the free cyanide ion, [CN$^-$], was simply calculated from the concentrations of the total cyanide, C_{CN^-}, and the total copper(I), $C_{Cu(I)}$, according to this equation: $[CN^-]=C_{CN^-}-4C_{Cu(I)}$.

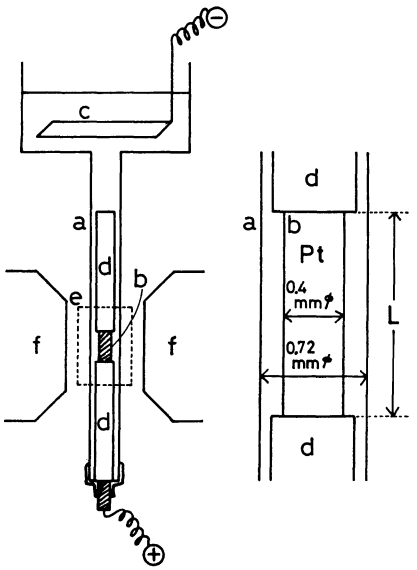

Fig. 1. Electrolysis cell for measurement of the ESR absorption intensity.
a: Quartz-glass tube, b: platinum-wire anode, c: platinum-plate cathode, d: polyethylene sheath, e. resonant cavity, f: electromagnet.

Results and Discussion

Relationship between the ESR Absorption Intensity and the Quantity of $Cu^{II}(CN)_4^{2-}$. When a potassium cyanide solution containing a small amount of copper(I) cyanide was electrolyzed in the cell shown in Fig. 1, an ESR absorption spectrum was observed, as shown in Fig. 2, which can be ascribed to the intermediate $Cu^{II}(CN)_4^{2-}$ ion.[1] Though copper(II) species other than $Cu^{II}(CN)_4^{2-}$ might possibly be formed during electrolysis, the ESR spectra did not show any evidence of such species at all under the experimental conditions in this work. In the following analysis, therefore, copper(II) is considered to be present almost totally as $Cu^{II}(CN)_4^{2-}$.

The signal intensity of the first-derivative spectrum can be regarded as proportional to the quantity of $Cu^{II}(CN)_4^{2-}$ formed,[5] because the spectrum exhibited the Lorentzian line-shape, because the peak positions did not vary with the intensity, and because the local difference in sensitivity due to the inequality of microwave field was negligible in the small anode compartment. On the basis of the above considerations, the signal intensity, I, was measured under different conditions at a fixed magnetic field, H_0, where the peak was the highest, as is shown in Fig. 2. In these experiments the conditions of the ESR spectrometer were kept strictly constant, and the unit scale (1 div) on the recorder chart was used as the unit of the signal intensity.

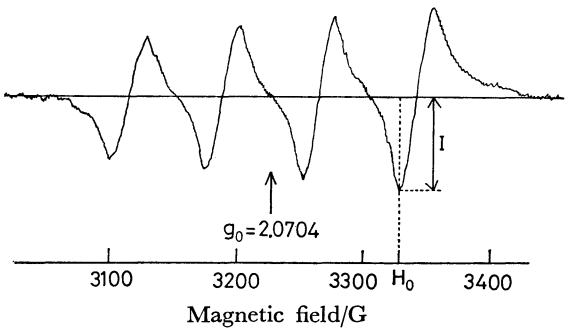

Fig. 2. ESR absorption spectrum $Cu^{II}(CN)_4^{2-}$.

Figure 3 shows a typical change in the ESR signal intensity after the switching-on and switching-off of the constant electrolysis current for a solution with a small $C_{Cu(I)}/C_{CN^-}$ ratio. The signal intensity was zero before starting electrolysis, since $Cu^{II}(CN)_4^{2-}$ was not present. When a constant anodic current was switched on, the intensity increased linearly with the time at first, and then reached a steady value. After the current was switched off, the intensity decreased, quickly at first and then slowly, to zero. Figure 4 shows the initial rate of increase in the signal intensity at the beginning of electrolysis, against the applied current. A proportionality is seen between them. It has been confirmed by other experiments that the initial rate of increase in the signal intensity is independent of the other conditions, *i.e.*, the concentrations of the free cyanide and the total copper(I), and the electrode length.

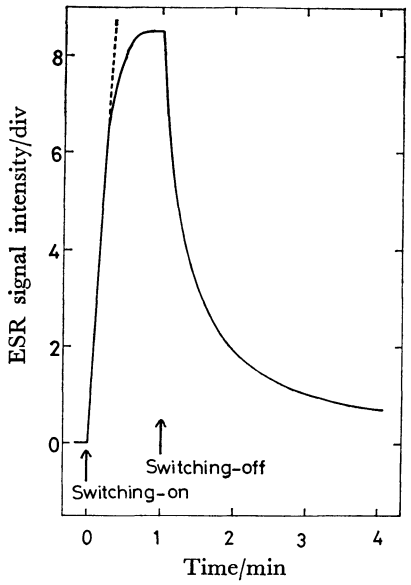

Fig. 3. Intensity of ESR absorption signal of $Cu^{II}(CN)_4^{2-}$ after switching-on and switching-off of the constant electrolysis current. (The unit intensity (1 div) corresponds to 1.55×10^{-9} mol of $Cu^{II}(CN)_4^{2-}$, *cf.* the text).
[CN⁻]: 3 M, $C_{Cu(I)}$: 0.1 M, current: 60 μA, electrode length: 6 mm.

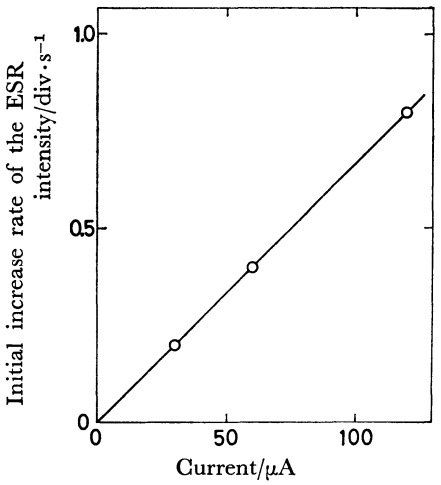

Fig. 4. Relationship between the initial increase rate of ESR signal intensity and the current.
[CN⁻]: 3 M, $C_{Cu(I)}$: 0.1 M, electrode length: 6 mm.

As a method for determining the quantity of a paramagnetic species from the ESR absorption intensity, Faraday's law has been applied by some workers. Hirasawa *et al.*[6] have applied this method to the formation of the anion radical of nitrobenzene, and Dohrmann and Gallussen,[7] to the formation of the copper(II) ion. A similar method is used in this work. The results shown in Figs. 3 and 4 indicate that at the beginning of electrolysis, the rate of the decomposition of $Cu^{II}(CN)_4^{2-}$ is negligible in comparison with the rate of the formation of $Cu^{II}(CN)_4^{2-}$, and that the current efficiency of the formation (Eq. 1) of $Cu^{II}(CN)_4^{2-}$ is almost 100%. Therefore, the quantity of $Cu^{II}(CN)_4^{2-}$, m, corresponding to the unit

intensity of the ESR signal is calculated from the slope of the line in Fig. 4, on the basis of Faraday's law, as follows:

$$m = 1.55 \times 10^{-9}\ \text{mol/div.} \quad (3)$$

It may reasonably be assumed that the concentration of the intermediate $Cu^{II}(CN)_4^{2-}$ is substantially uniform in the anode compartment along the length, L (Fig. 1), because the gap between the electrode surface and the glass wall is relatively small (0.16 mm), and because the current-density distribution may be nearly uniform due to the small current and the large electrolytic conductivity of the solution. For example, the concentration of $Cu^{II}(CN)_4^{2-}$ during the steady-state electrolysis shown in Fig. 3 is calculated to be 7.8×10^{-3} M by using the value, m, of Eq. 3 and the volume, $V=1.69\times10^{-3}$ cm^3, of the anode compartment. Kinetic analyses will be made on the above assumption in the following two sections. The validity of the assumption will be discussed in more detail in a later section.

Kinetics and Mechanism of the Decomposition of $Cu^{II}(CN)_4^{2-}$. In order to investigate the kinetics of the decomposition of $Cu^{II}(CN)_4^{2-}$, the decay of the ESR signal was followed after the electrolysis current has been switched off at certain steady state. The lower the CN^- concentration, the faster the signal decayed. Figure 5 shows the reciprocal of the signal intensity against the time for three different concentrations of CN^-. A linear relationship is found, indicating that the kinetics is second-order with respect to $Cu^{II}(CN)_4^{2-}$. Thus, the rate of the reaction, which is defined as the rate of the disappearance of $Cu^{II}(CN)_4^{2-}$, may be formulated as follows:

$$v = -\frac{d[Cu^{II}(CN)_4^{2-}]}{dt} = k_2[Cu^{II}(CN)_4^{2-}]^2. \quad (4)$$

The rate constant, k_2, is calculated from the slope of each line in Fig. 5 by using the "m" and "V" values, while log k_2 is plotted against log [CN^-] in Fig. 6. Since k_2 is found to be inversely proportional to the square of [CN^-], the rate equation, Eq. 4, can be

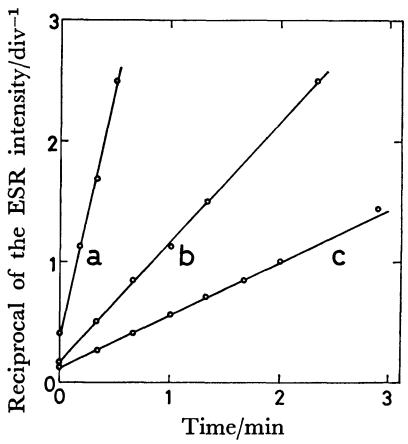

Fig. 5. Relationship between the reciprocal of ESR absorption signal intensity and time at different CN^- concentrations.
[CN^-]; a: 1 M, b: 2 M, c: 3 M, $C_{Cu(I)}$: 0.1 M, electrode length: 6 mm.

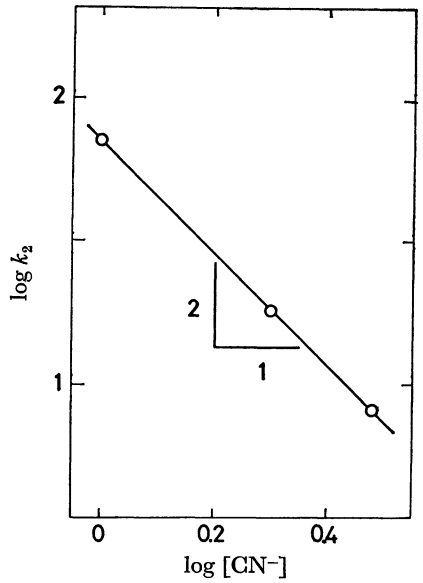

Fig. 6. Dependence of the second-order rate constant, $k_2(M^{-1}\,s^{-1})$ upon the CN^- concentration (M).

rewritten as Eq. 5, where k_0 is calculated to be 74 $M\cdot s^{-1}$:

$$v = k_0\frac{[Cu^{II}(CN)_4^{2-}]^2}{[CN^-]^2}. \quad (5)$$

Two types of reaction mechanisms can be considered, both of which are consistent with the rate equation, Eq. 5:

Mechanism A:

$$Cu^{II}(CN)_4^{2-} \overset{K_a}{\rightleftharpoons} Cu^{II}(CN)_3^- + CN^- \quad (6a)$$

$$2Cu^{II}(CN)_3^- \xrightarrow{k_a} 2Cu^{I}(CN)_2^- + (CN)_2 \quad (7a)$$

Mechanism B:

$$2Cu^{II}(CN)_4^{2-} \overset{K_a}{\rightleftharpoons} Cu^{II}_2(CN)_6^{2-} + 2CN^- \quad (6b)$$

$$Cu^{II}_2(CN)_6^{2-} \xrightarrow{k_b} 2Cu^{I}(CN)_2^- + (CN)_2 \quad (7b)$$

If the reaction, Eq. 6a or 6b, is in quasi-equilibrium when $[Cu^{II}(CN)_4^{2-}]\gg[Cu^{II}(CN)_3^-]$ or $[Cu^{II}(CN)_4^{2-}]\gg[Cu^{II}_2(CN)_6^{2-}]$, and if the reaction, Eq. 7a or 7b, is rate-determining, the rate equation may be described as follows:

$$v = k_aK_a^2\frac{[Cu^{II}(CN)_4^{2-}]^2}{[CN^-]^2}, \quad (8a)$$

or:

$$v = k_bK_b\frac{[Cu^{II}(CN)_4^{2-}]^2}{[CN^-]^2}. \quad (8b)$$

Here, K_a and K_b are the equilibrium constants of the reactions, Eqs. 6a and 6b, and k_a and k_b are the rate constants of the reactions, Eqs. 7a and 7b, respectively. Both Eqs. 8a and 8b agree with the experimental rate equation, Eq. 5. At present, it is not possible to decide which of the two mechanisms is correct. Another experiment has been made on this point, however, and a further discussion will be presented in a succeeding paper.

Since cyano copper(I) complexes are labile,[8] the following equilibrium may always exist:

$$Cu^{I}(CN)_2^- + 2CN^- \longrightarrow Cu^{I}(CN)_4^{3-}. \quad (9)$$

During a steady-state electrolysis, the over-all reaction may proceed through the reaction cycle of Eqs. 1, 6a, 7a, and 9, or Eqs. 1, 6b, 7b, and 9.

Kinetics during Steady-state Electrolysis. In order to confirm the rate equation, Eq. 5, the steady-state intensity of the ESR signal was measured under different conditions. Figures 7, 8, and 9 show the dependencies of the signal intensity, I, upon the anodic current, j; the electrode length, L, and the concentration of the free cyanide ion, [CN⁻]. It can be noticed from these figures that the signal intensity is proportional to $j^{1/2}$, $L^{1/2}$, and [CN⁻].

It has been assumed that the intermediate $Cu^{II}(CN)_4^{2-}$ exists uniformly in the anode compartment whose volume is $V=\pi(R^2-r^2)L$, where R is the inner radius of the quartz-glass tube and where r is the radius of the platinum-wire electrode. In a steady state when the rates of the formation and decomposition of the intermediate $Cu^{II}(CN)_4^{2-}$ are equal, the following expression should hold:

$$\frac{j}{F} = k_0 \frac{[Cu^{II}(CN)_4^{2-}]^2}{[CN^-]^2} \pi(R^2-r^2)L. \quad (10)$$

On the other hand, the steady-state intensity of the ESR signal is expressed by Eq. 11:

$$I = \frac{1}{m}[Cu^{II}(CN)_4^{2-}]\pi(R^2-r^2)L. \quad (11)$$

By combining Eqs. 10 and 11, the following equation is obtained:

$$I = \frac{1}{m}\left\{\frac{\pi(R^2-r^2)}{k_0 F}\right\}^{1/2} \cdot j^{1/2}L^{1/2}[CN^-]. \quad (12)$$

Thus, the intensity should be proportional to $j^{1/2}$, $L^{1/2}$, and [CN⁻]. These relationships are satisfied experimentally, as has been mentioned above. The rate constant, k_0, is calculated to be 60 $M \cdot s^{-1}$ from the results of Figs. 7, 8, and 9 on the basis of Eq. 12. This value is in satisfactory agreement with the value, 74 $M \cdot s^{-1}$, obtained in the previous section.

Distribution of the Concentration of $Cu^{II}(CN)_4^{2-}$ in the Anode Compartment. Kinetic analyses have been made in the preceding sections on the assumption that the concentration of $Cu^{II}(CN)_4^{2-}$ was uniform in the anode compartment. The validity of this assumption will now be discussed.

It is known that cyanogen is primarily formed in the anodic oxidation of the cyanide ion and is then hydrolyzed according to Eq. 13:[9]

$$(CN)_2 + H_2O \longrightarrow HCN + HOCN. \quad (13)$$

When the concentration of CN⁻ is sufficiently high, the hydrogen cyanide polymerizes, according to Eq. 14, to give a brown polymer, which is called "azulmin":[10]

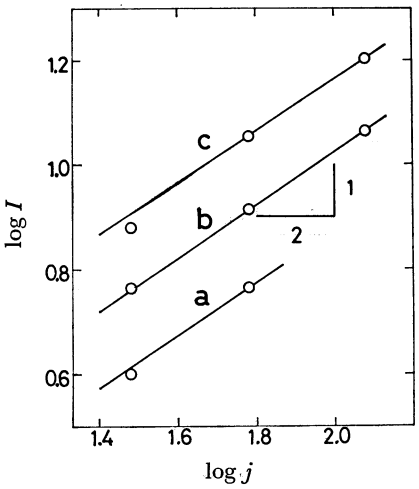

Fig. 7. Relationship between the logarithm of steady-state ESR intensity (div) and the logarithm of current (μA).
[CN⁻]: 3 M, $C_{Cu(I)}$: 0.1 M, electrode length; a: 3 mm, b: 6 mm, c: 12 mm.

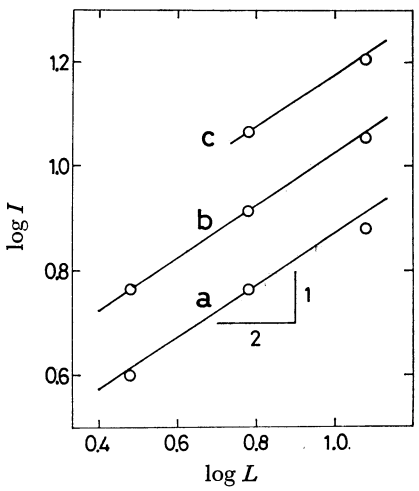

Fig. 8. Relationship between the logarithm of steady-state ESR intensity (div) and the logarithm of electrode length (mm).
[CN⁻]: 3 M, $C_{Cu(I)}$: 0.1 M, current; a: 30 μA, b: 60 μA, c: 120 μA.

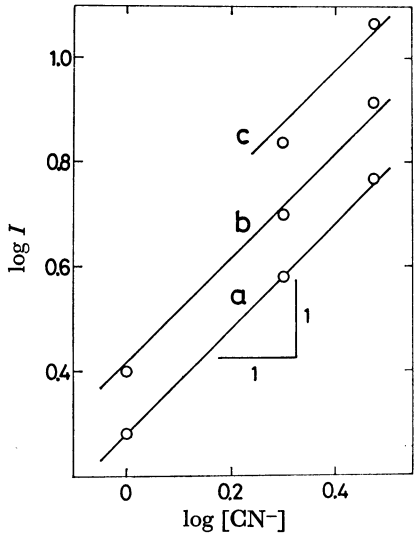

Fig. 9. Relationship between the logarithm of steady-state ESR intensity (div) and the logarithm of CN⁻ concentration (M).
$C_{Cu(I)}$: 0.1 M, electrode length: 6 mm, current; a: 30 μA, b: 60 μA, c: 120 μA.

$$x\mathrm{HCN} \longrightarrow (\mathrm{HCN})_x. \quad (14)$$

Such a brown polymer was often observed after long-time electrolysis in the present work, too. The formation of the brown polymer was almost uniform along the length of the anode, indicating that the current-density distribution was almost uniform.

The distribution of the concentration of $Cu^{II}(CN)_4^{2-}$ in the radial direction, *i.e.*, the direction normal to the electrode surface, can be calculated for steady-state electrolysis by using the rate equation, Eq. 4, and an appropriate differential equation. If the x-axis is chosen in the radical direction, with the origin at the electrode surface, and if an approximation of the linear diffusion is made, a differential equation with respect to the concentration, C, of $Cu^{II}(CN)_4^{2-}$ is established as follows:

$$\frac{\partial C}{\partial t} = D\frac{\partial^2 C}{\partial x^2} - k_2C^2. \quad (15)$$

Here, D is the diffusion coefficient of $Cu^{II}(CN)_4^{2-}$, while k_2 is the rate constant in Eq. 4. At a steady state, when $\partial C/\partial t=0$, Eq. 15 gives Eq. 16:

$$\frac{d^2C}{dx^2} - \frac{k_2}{D}C^2 = 0. \quad (16)$$

Boundary conditions, Eqs. 17 and 18, hold:

$$\frac{dC}{dx} = -\frac{J}{DF} \quad \text{and } C=C_0 \text{ at } x=0 \quad (17)$$

$$\frac{dC}{dx} = 0 \quad \text{and } C=C_a \text{ at } x=a \quad (18)$$

where J is the current density, where a is the distance between the electrode surface and the glass wall ($a=R-r$), and where the subscripts 0 and a indicate the electrode surface and the glass wall respectively. By integrating Eq. 16 under the conditions of Eqs. 17 and 18, the following equations are derived:

$$\frac{dC}{dx} = -\sqrt{\frac{2k_2}{3D}(C^3-C_a^3)} \quad (19)$$

$$C_0^3 - C_a^3 = \frac{3}{2}\frac{J^2}{k_2DF^2}. \quad (20)$$

The integration of Eq. 19 gives Eq. 21:

$$\frac{1}{\sqrt[4]{3}}F\left\{\arccos\frac{\frac{C}{C_a}-(\sqrt{3}+1)}{\frac{C}{C_a}+(\sqrt{3}-1)}, \frac{\sqrt{3}-1}{2\sqrt{2}}\right\} = \left(\frac{2k_2C_a}{3D}\right)^{1/2}(a-x), \quad (21)$$

where $F(\varphi, k)$ indicates the elliptic integral of the first kind.[11] The concentration distribution can be calculated numerically from Eqs. 20 and 21. A typical example is shown by Curve a in Fig. 10, in which the values of $k_0=74\ \mathrm{M\cdot s^{-1}}$ and $D=10^{-5}\ \mathrm{cm^2\cdot s^{-1}}$† are used.

The horizontal line (Curve b) shows the average concentration, which was obtained from the ESR absorption intensity. The fact that Curve a lies near

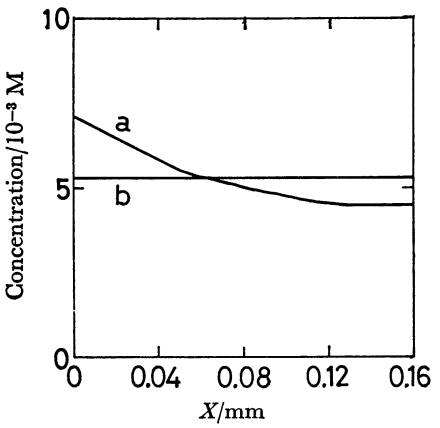

Fig. 10. Calculated concentration distribution (a) of $Cu^{II}(CN)_4^{2-}$ in the cell, compared with the experimentally observed average-value (b).
[CN⁻]: 3 M, $C_{Cu(I)}$: 0.1 M, electrode length: 6 mm, current: 30 μA.

Curve b shows the approximate validity of the assumption that the $Cu^{II}(CN)_4^{2-}$ concentration is uniform in the radial direction in the cell.

Comparison with the Kinetics and Mechanisms of the Chemical Reaction between Cu^{2+} and CN^- Ions. It is known that the copper(II) ion reacts with the cyanide ion in an aqueous solution to give copper(II) cyanide as a yellowish-brown precipitate, which then decomposes to copper(I) cyanide and cyanogen, according to Eqs. 22 and 23:[14,15]

$$Cu^{2+} + 2CN^- \longrightarrow Cu^{II}(CN)_2 \quad (22)$$

$$2Cu^{II}(CN)_2 \longrightarrow 2Cu^{I}CN + (CN)_2. \quad (23)$$

The cyanogen thus formed is evolved as a gas from an acidic solution, or it is decomposed in an alkaline solution as follows:

$$(CN)_2 + 2OH^- \longrightarrow CN^- + OCN^- + H_2O. \quad (24)$$

When the concentration of the copper(II) ion is much lower than that of the cyanide ion, not copper(II) cyanide but a purple intermediate is formed, which then gives cyanogen and a copper(I) species. Several papers have reported about this purple compound.[16–19]

The rate of the reaction between the copper(II) ion and the cyanide ion is too high under ordinary conditions to be measured by conventional methods. Duke and Courtney[20] have used the ammine copper (II) complex to diminish the reaction rate in their kinetic study, while Tanaka *et al.*[21] have used the ethylenediaminetetraacetatocopper(II) complex. Bjerrum *et al.*[22,23] have studied the kinetics in a methanol–water mixture at a low temperature. These three groups of workers have, from their kinetic considerations, expected the existence of $Cu^{II}(CN)_4^{2-}$ as an intermediate. From their measurements of ESR and optical spectra, Longo and Buch[24] have concluded the purple intermediate to be $Cu^{II}(CN)_4^{2-}$ with a square-planar configuration.

Nord and Matthes[25] have applied the stopped-flow technique to the reaction between the copper(II) ion and the cyanide ion in aqueous solutions at ambient temperatures. Thus by following the concentration of

† This value is estimated from the diffusion coefficients of Cu^{2+} ($D=0.72\times10^{-5}\ \mathrm{cm^2\cdot s^{-1}}$)[12] and $Cu^{II}(NH_3)_4^{2+}$ ($D=0.95\times10^{-5}\ \mathrm{cm^2\cdot s^{-1}}$),[13] both of which have the same square-planar configuration as $Cu^{II}(CN)_4^{2-}$.

the intermediate $Cu^{II}(CN)_4^{2-}$ by using an optical spectrometer and a oscilloscope, they obtained a rate equation, Eq. 25, from which they have proposed a reaction mechanism, Eqs. 26 and 27, the latter being rate-determining:

$$v = k_1 \frac{[Cu^{II}(CN)_4^{2-}]^2}{[CN^-]} \quad (25)$$

$$Cu^{II}(CN)_4^{2-} \rightleftharpoons Cu^{II}(CN)_3^- + CN^- \quad (26)$$

$$Cu^{II}(CN)_4^{2-} + Cu^{II}(CN)_3^- \longrightarrow \text{Product.} \quad (27)$$

There is an agreement between their work and ours in that the reaction rate is proportional to the square of $[Cu^{II}(CN)_4^{2-}]$. However, there is a disagreement in the dependency upon $[CN^-]$.

Baxendale and Westcott[26] have studied the kinetics at rather low pH values, where the concentration of the free cyanide ion is so small that the reaction rate is relatively small and can easily be measured. Thus, they followed the change in the concentration of the reaction product, $Cu^I(CN)_2^-$, by means of a UV spectrometer, and obtained the result that the reaction rate is proportional to the 6th power of $[CN^-]$ and to the square of $[Cu^{2+}]$. From this kinetic data, they have proposed the following mechanism, in which the Eq. 29 reaction is rate-determining:

$$Cu^{2+} + 3CN^- \rightleftharpoons Cu^{II}(CN)_3^- \quad (28)$$

$$2Cu^{II}(CN)_3^- \longrightarrow 2Cu^I(CN)_2^- + (CN)_2. \quad (29)$$

Their result is compatible with that of our present work. Equation 29 is the same as Eq. 7a, while their kinetic data can also be explained by the formation of $Cu^{II}_2(CN)_6^{2-}$, followed by the rate-determining reaction, Eq. 7b.

A more detailed discussion of the kinetics and the mechanisms of the chemical reaction between the copper(II) ion and the cyanide ion will be presented in a succeeding paper.

We would like to thank Professor Saburo Kako for his helpful discussions, and Mr. Hideo Fujita for his assistance in measuring the ESR spectra. The present work was partly supported by a Grant-in-Aid for Scientific Research (Environmental Science) from the Ministry of Education, Science and Culture (No. 403523).

References

1) Part III of this series: S. Yoshimura, A. Katagiri, Y. Deguchi, and S. Yoshizawa, *Bull. Chem. Soc. Jpn.*, **53**, 2434 (1980).
2) S. Yoshimura, A. Katagiri, and S. Yoshizawa, *Denki Kagaku*, **47**, 360 (1979).
3) S. Yoshimura, A. Katagiri, and S. Yoshizawa, *Denki Kagaku*, **47**, 488 (1979).
4) R. A. Penneman and L. H. Jones, *J. Chem. Phys.*, **24**, 293 (1956).
5) "Jikken Kagaku Kōza," ed by The Chemical Society of Japan, Maruzen, Tokyo (1967), Suppl. Vol. 13, p. 425.
6) R. Hirasawa, T. Mukaibo, H. Hasegawa, N. Odan, and T. Murayama, *J. Phys. Chem.*, **72**, 2541 (1968).
7) J. K. Dohrmann and F. Gallussen, *Ber. Bunsenges. Phys. Chem.*, **75**, 432 (1971).
8) A. G. MacDiarmid and N. F. Hall, *J. Am. Chem. Soc.*, **76**, 4222 (1954).
9) R. A. Nauman, *Z. Elektrochem.*, **16**, 722 (1910).
10) H. Schmidt and H. Meinert, *Z. Anorg. Allg. Chem.*, **293**, 214 (1959).
11) S. Moriguchi, K. Udagawa, and S. Hitotsumatsu, "Sugaku Koshiki I," Iwanami Shoten, Tokyo (1956), p. 148.
12) "Denki Kagaku Benran," ed by The Electrochemical Society of Japan, Maruzen, Tokyo (1964), p. 95.
13) I. M. Kolthoff and J. J. Lingane, "Polarography," Interscience (1952), p. 494.
14) "Gmelin Handbuch," Cu[B] 60, Verlag Chemie GmbH (1965), p. 1447.
15) T. Chitani, "Muki Kagaku," Sangyō Tosho, Tokyo (1964), p. 479.
16) A. G. Sharpe, "The Chemistry of Cyano Complexes of the Transition Metals," Academic Press (1976), p. 271.
17) B. N. Chadwick and A. G. Sharpe, "Advances in Inorganic Chemistry and Radiochemistry," (1966), Vol. 8 p. 83.
18) W. P. Griffith, *Quart. Rev. (London)*, **16**, 188 (1962).
19) A. Glasner and K. R. S. Asher, *J. Chem. Soc.*, **1949**, 3296.
20) F. R. Duke and W. G. Courtney, *J. Phys. Chem.*, **56**, 19 (1952).
21) N. Tanaka, M. Kamada, and T. Murayama, *Bull. Chem. Soc. Jpn.*, **31**, 895 (1959).
22) O. Mønsted and J. Bjerrum, *Acta Chem. Scand.*, **21**, 1116 (1967).
23) R. Paterson and J. Bjerrum, *Acta Chem. Scand.*, **19**, 729 (1965).
24) A. Longo and T. Buch, *Inorg. Chem.*, **6**, 556 (1967).
25) G. Nord and H. Matthes, *Acta Chem. Scand.*, **A28**, 13 (1974).
26) J. H. Baxendale and D. T. Westcott, *J. Chem. Soc.*, **1959**, 2347.